



Cite this: DOI: 10.1039/d0sc05133k

All publication charges for this article have been paid for by the Royal Society of Chemistry

Received 17th September 2020  
Accepted 31st October 2020

DOI: 10.1039/d0sc05133k

rsc.li/chemical-science

## Cross dehydrogenative C–O coupling catalysed by a catenane-coordinated copper(i)<sup>†</sup>

Lihui Zhu,<sup>a</sup> Jiasheng Li,<sup>a</sup> Jun Yang<sup>id</sup><sup>a</sup> and Ho Yu Au-Yeung<sup>id</sup><sup>\*ab</sup>

Catalytic activity of copper(i) complexes supported by phenanthroline-containing catenane ligands towards a new C(sp<sup>3</sup>)–O dehydrogenative cross-coupling of phenols and bromodicarbonyls is reported. As the phenanthrolines are interlocked by the strong and flexible mechanical bond in the catenane, the active catalyst with an open copper coordination site can be revealed only transiently and the stable, coordinatively saturated Cu(i) pre-catalyst is quickly regenerated after substrate transformation. Compared with a control Cu(i) complex supported by non-interlocked phenanthrolines, the catenane-supported Cu(i) is highly efficient with a broad substrate scope, and can be applied in gram-scale transformations without a significant loss of the catalytic activity. This work demonstrates the advantages of the catenane ligands that provide a dynamic and responsive copper coordination sphere, highlighting the potential of the mechanical bond as a design element in transition metal catalyst development.

## Introduction

Copper is an attractive alternative to precious metals in transition metal-catalysed cross couplings because of its Earth abundance and relatively low price.<sup>1</sup> Mechanistically, copper-catalysed couplings are very diverse and can involve Cu(i)/Cu(II)/Cu(III) intermediates and different pathways such as double-electron oxidative addition–reductive elimination, electrophilic substitution, radical substitution and bimetallic reduction.<sup>2</sup> The optimal coordination environment for the copper at various stages of the coupling could be very different, and a ligand that can accommodate the changing copper coordination characteristics in the catalytic cycle will be key to the development of an efficient copper catalyst. Generally, an open coordination site is required for substrate coordination and transformation, but a coordinatively saturated copper at the resting state can prolong the catalyst lifetime and minimise off-target reactivity.<sup>3</sup> For a coordinatively saturated copper precatalyst, dissociation of the parent ligand will precede substrate coordination to produce an active catalyst.<sup>4</sup> However, the presence of an open coordination site can also subject the active catalyst to unproductive side reactions, and regenerating the stable precatalyst by intermolecular coordination of the dissociated parent ligand may not be kinetically favourable.<sup>5</sup> While stable copper complexes with an open coordination site can be obtained by using low dentate, sterically

demanding ligands, bulkiness of the ligands will have to be carefully balanced to maintain catalytic activity.<sup>6</sup> Another approach would be the use of a chelating, hemilabile ligand consists of both strongly and weakly coordinating donors, in which the former acts as an anchor to the copper centre and the latter can dissociate and re-coordinate easily for substrate transformation and pre-catalyst regeneration.<sup>7</sup>

In contrast to these strategies that focus only on designing an optimal ligand covalent framework, we propose that a responsive copper coordination sphere can be attained by the use of mechanically interlocked ligands for transiently revealing an open coordination site for catalysis, while maintaining a saturated coordination at the resting state for a good stability.<sup>8</sup> For example, a 4-coordinate, tetrahedral copper(i) supported by a catenane derived from two interlocked, phenanthroline-containing macrocycles is highly stable because of the kinetic stabilisation from the strong mechanical bond.<sup>9</sup> Flexibility of the mechanical bond could also result in a change of the catenane conformation in response to an external stimulus,<sup>10</sup> and an open copper coordination site could be temporarily revealed for catalysis. Because the ligands are mechanically bonded, intramolecular re-coordination of any dissociated donor to regenerate the stable, tetrahedral precatalyst will also be kinetically favourable. The mechanical bond can thus prevent the active catalyst from participating non-productive side reactions, prolong the catalyst lifetime, and possibly stabilise reactive intermediates and facilitate product dissociation to effect a faster turnover (Fig. 1).<sup>11</sup> In spite of these potential advantages and that copper(i) has been one most studied metal template in the synthesis of various types of mechanically interlocked molecules (MIMs),<sup>12</sup> the use of copper-coordinated MIMs for catalysis is yet to be reported.

<sup>a</sup>Department of Chemistry, The University of Hong Kong, Pokfulam Road, Hong Kong, P. R. China. E-mail: hoyuay@hku.hk

<sup>b</sup>State Key Laboratory of Synthetic Chemistry, The University of Hong Kong, Pokfulam Road, Hong Kong, P. R. China

<sup>†</sup> Electronic supplementary information (ESI) available: Experimental procedures, characterization data, computational details, HRMS spectrum and <sup>1</sup>H, <sup>13</sup>C NMR spectra. See DOI: 10.1039/d0sc05133k

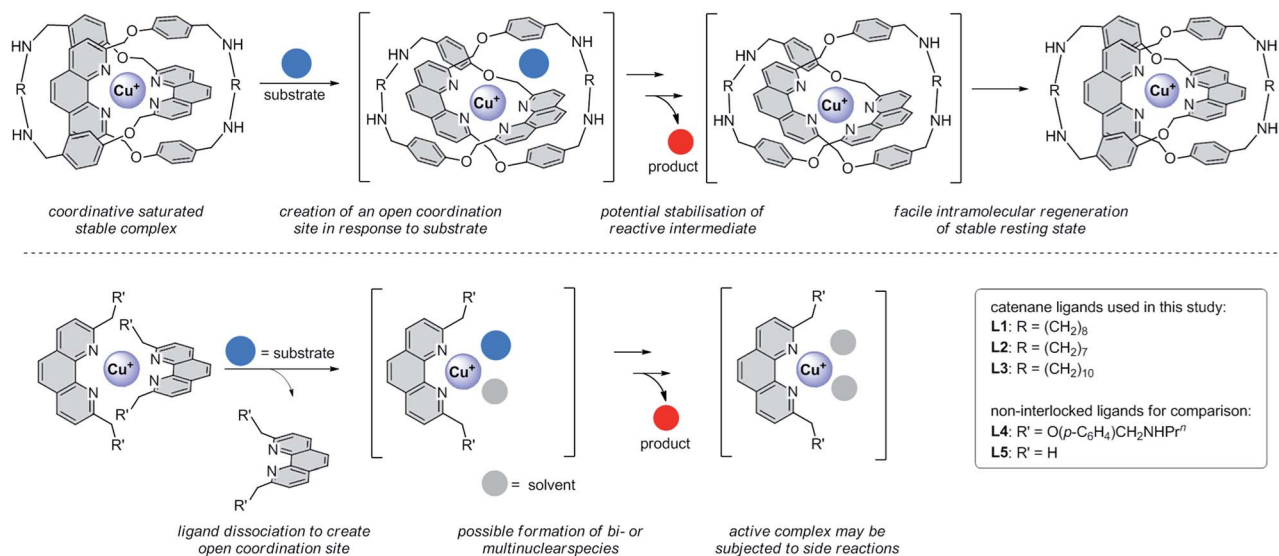


Here we report that Cu(I) complexes supported by a catenane consists of two interlocked, phenanthroline-derived macrocycles can catalyse a new cross dehydrogenative C(sp<sup>3</sup>)-O coupling (CDC) between phenols and bromodicarbonyls. The catenane-supported Cu(I) is highly efficient with a broad substrate scope, and can be applied in a gram-scale synthesis without compromising the catalytic activity. Of note, C(sp<sup>3</sup>)-O cross dehydrogenative coupling, in particular with phenolic substrates, is the most challenging among various CDC due to the strong, non-selective oxidation tendency and propensity of other side reactions of phenols such as hydroxylation and C-oxidation.<sup>13,14</sup> Currently, there are only few reports of C(sp<sup>2</sup>)-O dehydrogenative coupling of phenols with anilines,<sup>15</sup> formamides,<sup>16</sup> acrylates<sup>17</sup> and catechols.<sup>18</sup> C(sp<sup>3</sup>)-O cross coupling is even more challenging, and the use of a hypervalent iodine oxidant<sup>19</sup> or a metal-free condition are among the few reported examples of C(sp<sup>3</sup>)-O cross coupling in the literatures.<sup>20</sup> Preliminary mechanistic studies on the catenane-supported Cu(I) suggest the CDC involves a mononuclear, radical-involving pathway. Removing the mechanical bond in the Cu(I) catalyst not only resulted in a much lower catalytic activity, but also the CDC was found likely to proceed *via* binuclear species. The good stability and catalytic activity of the interlocked copper catalysts thus demonstrate the huge potential and opportunities in exploring the ligand topological space for developing new generations of copper catalysts.

## Results and discussion

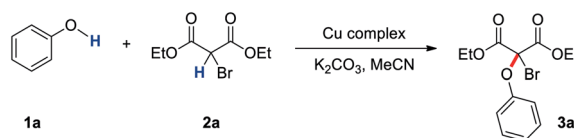
As part of our program on exploring the chemistry of mechanical bond,<sup>21</sup> we discovered that the dehydrogenative coupling of phenol **1a** and diethyl bromomalonate **2a** can be effectively

catalysed by 5 mol% of [Cu(L1)]PF<sub>6</sub> in the presence of 2 eq. of K<sub>2</sub>CO<sub>3</sub> to give **3a** in 80% yield (Table 1, entry 1). Scavenging other possible copper species by virtue of the very strong Cu(I) affinity of an additional 1 mol% or 5 mol% of L1 resulted in a similar yield of **3a** in 77% and 78% respectively (Table 1, entries 2 and 3).<sup>9b</sup> Furthermore, when [Cu(L1)]PF<sub>6</sub> was replaced by [Cu(MeCN)<sub>4</sub>]PF<sub>6</sub>, yield of **3a** decreased to 44% (Table 1, entry 4), showing that the observed catalytic effect was due to [Cu(L1)]PF<sub>6</sub>. Other copper complexes also gave **3a** in only *ca.* 30–50% yields, reinforcing the effect of the interlocked ligand on the coupling reaction (Table S2†). LC-ESI-MS analysis of the mixture after the CDC showed [Cu(L1)]<sup>+</sup> (*m/z* = 1184.1) remained as the only detectable copper-containing species in the system (Fig. S1†), supporting that the catenane-coordinated copper(I) is stable yet catalytically active. On the other hand, with a slightly tighter mechanical bond, [Cu(L2)]PF<sub>6</sub> gave **3a** in only 52% yield under the same condition. In contrast, a 77% yield of **3a** was observed when the less tight [Cu(L3)]PF<sub>6</sub> was used as the catalyst (Table 1, entries 5 and 6). These results agree with our proposal that a responsive copper coordination sphere for switching between the catalytically active and the stable pre-catalytic states can be obtained by the use of a strong and flexible mechanical bond. In fact, stabilisation of a metal centre by mechanically bonded ligands is kinetic in nature and originates from the increased barrier of the reorganization and complete dissociation of the interlocked ligands. Steric hindrance at the metal center is not necessarily enhanced by the presence of mechanical bond.<sup>9a,b</sup> It is therefore possible to tune the ligand dissociation and reorganisation kinetics, and hence the metal reactivity, by a careful tuning of the tightness of the mechanical bond in the interlocked ligands,<sup>22</sup> highlighting an unique feature of mechanical bond in ligand design for



**Fig. 1** Comparison of a Cu(I) catalysts supported by a catenane ligand (top) and non-interlocked ligands (bottom). For complexes supported by catenane ligands, the stable resting state can change its coordination environment for substrate transformation and be regenerated by facile intramolecular coordination of the dissociated ligand. On the other hand, re-coordination of dissociated ligand that is non-interlocked will be kinetically less favourable. Empty coordination sites created after ligand dissociation may be filled by solvents and bi/multinuclear complexes could be formed. The active complex may be more susceptible to side reactions with a shorter lifetime.



Table 1 Screening of the CDC reaction<sup>a</sup>

Entry	Cu complex	K <sub>2</sub> CO <sub>3</sub>	Temp	Yield of 3a <sup>b</sup>
1	5 mol% [Cu(L1)]PF <sub>6</sub>	2 eq.	25 °C	80%
2	5 mol% [Cu(L1)]PF <sub>6</sub> + 1 mol% L1	2 eq.	25 °C	77%
3	5 mol% [Cu(L1)]PF <sub>6</sub> + 5 mol% L1	2 eq.	25 °C	78%
4	5 mol% [Cu(MeCN) <sub>4</sub> ]PF <sub>6</sub>	2 eq.	25 °C	44%
5	5 mol% [Cu(L2)]PF <sub>6</sub>	2 eq.	25 °C	52%
6	5 mol% [Cu(L3)]PF <sub>6</sub>	2 eq.	25 °C	77%
7	2 mol% [Cu(L1)]PF <sub>6</sub>	2 eq.	25 °C	78%
8	1 mol% [Cu(L1)]PF <sub>6</sub>	2 eq.	25 °C	77%
9	1 mol% [Cu(L1)]PF <sub>6</sub> (under argon)	2 eq.	25 °C	77%
10	1 mol% [Cu(L1)]PF <sub>6</sub>	0 eq.	25 °C	28%
11	1 mol% [Cu(L1)]PF <sub>6</sub>	2 eq.	50 °C	92% <sup>c</sup>
12 <sup>d</sup>	0.005 mol% [Cu(L1)]PF <sub>6</sub>	2 eq.	50 °C	83%
13	1 mol% [Cu(L1)]PF <sub>6</sub> + 1 eq. TEMPO	2 eq.	50 °C	26%
14	1 mol% [Cu(L4) <sub>2</sub> ]PF <sub>6</sub>	2 eq.	50 °C	71%
15	1 mol% [Cu(L5) <sub>2</sub> ]PF <sub>6</sub>	2 eq.	50 °C	42%
16	1 mol% [Cu(L4) <sub>2</sub> ]PF <sub>6</sub> + 1 eq. TEMPO	2 eq.	50 °C	55%
17 <sup>d</sup>	0.005 mol% [Cu(L4) <sub>2</sub> ]PF <sub>6</sub>	2 eq.	50 °C	35%
18	1 mol% [Cu(L5) <sub>2</sub> ]PF <sub>6</sub> + 1 eq. TEMPO	2 eq.	50 °C	70%

<sup>a</sup> Reaction was conducted with 1a (0.1 mmol) and 2a (0.22 mmol) in 0.5 mL MeCN for 24 hours. <sup>b</sup> Determined by <sup>1</sup>H NMR using 1,3,5-trimethoxybenzene as internal standard. <sup>c</sup> Isolated yield = 90%. <sup>d</sup> With 0.47 g (5 mmol) 1a and 1.76 g (11 mmol) 2a for 72 hours.

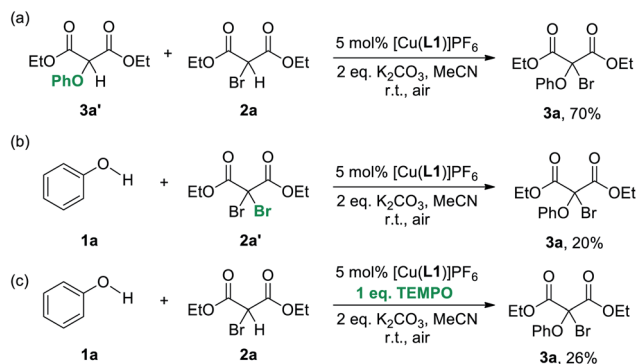
transition metal catalyst development. Other unique properties of MIMs that have also been exploited for catalytic applications include co-conformation switching of rotaxanes for switchable catalysis,<sup>23,24</sup> topological chirality as the chiral element in asymmetric catalysis,<sup>25</sup> and the strong binding affinity of an interlocked host for catalyst activation.<sup>26</sup> Together with this work that demonstrates the use of the strong and flexible mechanical bond for a dynamic control of the copper coordination site, it is clear that mechanical bond can offer many new opportunities in catalyst design.

Optimisation of the CDC showed that reducing the catalyst loading to as low as 1 mol% did not significantly affect the catalytic efficiency (Table 1, entries 7 and 8). This is in great contrast to most other copper-catalysed reactions, in which a low catalyst loading would often lead to a decrease in the product yield (see below), suggesting that the mechanical bond in L1 could stabilise the pre-catalytic state and prohibit non-productive side reactions. Consistent with this, the CDC can be performed under air, and protecting the reaction under argon had no significant effect on the product yield (Table 1, entry 9). This also suggests that 2a is the internal oxidant, which was confirmed by the presence of diethyl malonate in the product mixture (Fig. S6†). It was found that K<sub>2</sub>CO<sub>3</sub> is essential and eliminating the base from the reaction resulted in only 28% of 3a (Table 1, entry 10 and see ESI for more screening details†). Further optimising the reaction condition by increasing the temperature to 50 °C and using 1 mol% of [Cu(L1)]PF<sub>6</sub> with 2 eq. of K<sub>2</sub>CO<sub>3</sub> in a 24-hour reaction gave 3a in a good yield of 92%

(Table 1, entry 11). Moreover, loading of [Cu(L1)]PF<sub>6</sub> can be further lowered down to 0.005 mol% in a gram-scale transformation without compromising the catalytic efficiency (Table 1, entry 12). It is worth noting that L1 and related catenane ligands can also be obtained in gram-scale in spite of its non-trivial topology (see ESI for details†),<sup>27</sup> demonstrating the practical applicability of these interlocked ligands in transition metal catalysis.

Possible intermediates involved in the CDC were also studied. First, a reaction of 1a and 2a catalysed by [Cu(L1)]PF<sub>6</sub> at a reaction time of 30 min was analysed by <sup>1</sup>H NMR, which showed the presence of 3a and diethyl phenoxymalonate 3a' in ca. 10% and 70% yield respectively (Fig. S4†). As the reaction proceeded, amount of 3a continued to increase while that of 3a' decreased, and the reaction was completed after ~20 hours. These results led us to propose that formation of 3a is preceded by a nucleophilic substitution of 2a by 1a that gives 3a', which is also consistent with the essential role of K<sub>2</sub>CO<sub>3</sub> in the CDC. Indeed, an independent reaction between 2a and 3a' with 5 mol% [Cu(L1)]PF<sub>6</sub> at room temperature gave 3a in 70% yield, confirming that 3a can be formed from 3a' under the CDC condition (Scheme 1a). The reaction between 1a and *gem*-dibromodimethylmalonate 2a' was also tested, but 3a was formed in a low yield of 20%, showing that the CDC may not involve bromodimethylmalonate disproportionation (Scheme 1b).<sup>28</sup> Furthermore, the presence of 1 eq. of the radical scavenger 2,2,6,6-tetramethylpiperidine-1-oxyl (TEMPO) led to a sharp decrease in the yield of 3a to 26% (along with 3a' in 65%), suggesting that





**Scheme 1** Control reactions for studying possible intermediates involved in the CDC: (a) phenol (**1a**) was replaced by diethyl phenoxymalonate (**3a'**) that showed the formation of CDC product is preceded by a  $\text{S}_{\text{N}}$  reaction; (b) diethyl bromomalonate (**2a**) was replaced by diethyl dibromomalonate (**2a'**) that showed the CDC did not involve disproportionation of **2a**; (c) 1 eq. of TEMPO was added that showed the CDC catalysed by the catenane-supported Cu(I) could involve a radical species.

radicals may be involved in the reaction (Table 1, entry 13 and Scheme 1c). Although the formation of a copper-TEMPO complex that leads to the formation of non-CDC products could be another plausible reason for the reduced yield of **3a**,<sup>29</sup> no product other than **3a'** from the  $\text{S}_{\text{N}}$  reaction of **1a** and **2a** was identified. The highly preorganised phenanthrolines in **L1** also suggest that regenerating the stable  $[\text{Cu}(\text{L1})]^+$  from any transient, **L1**-supported copper-TEMPO complex will be kinetically favourable. Further  $^1\text{H}$  NMR and ESI-MS studies on  $[\text{Cu}(\text{L1})]\text{PF}_6$  in the presence of 50 eq. of TEMPO also showed no formation of any copper-TEMPO complex (Fig. S2 and S7†). On the other hand, generation of an alkyl radical from the corresponding halide with a  $\text{Cu}^{\text{I}}$  supported by chelating N-based ligands is well-accepted in copper-catalysed atom transfer radical addition and polymerization reactions.<sup>3</sup> Our initial DFT studies indeed showed that the formation of  $[\text{Cu}^{\text{II}}(\text{L1})\text{Br}]^+$  along with  $[\text{CH}(\text{COOEt})_2]^{\cdot}$  radical is viable with an energy difference of  $6.53 \text{ kcal mol}^{-1}$ , suggesting that the coupling product could be formed from a radical substitution involving  $[\text{C}(\text{OPh})(\text{COOEt})_2]^{\cdot}$  radical (Fig. 2). Although the large molecular size of the copper catenanes would impose a huge demand on a high-level computational study and our mechanistic study remains preliminary, it would be kinetically improbable for the interlocked phenanthrolines in **L1** to completely dissociate and formation of bi/multinuclear species are likely to be irrelevant.

Roles of the mechanical bond in  $[\text{Cu}(\text{L1})]\text{PF}_6$  was further studied by comparing with the CDC that employed the non-interlocked  $[\text{Cu}(\text{L4})_2]\text{PF}_6$  and  $[\text{Cu}(\text{L5})_2]\text{PF}_6$ . A lower yield of **3a** in 71% and 42%, as compared with that of 92% for  $[\text{Cu}(\text{L1})]\text{PF}_6$ , was observed when 1 mol% of  $[\text{Cu}(\text{L4})_2]\text{PF}_6$  and  $[\text{Cu}(\text{L5})_2]\text{PF}_6$  was used respectively under the optimised condition (Table 1, entries 14 and 15). While the addition of 1 eq. of TEMPO had significantly lowered the yield of **3a** by 66% in the case of  $[\text{Cu}(\text{L1})]\text{PF}_6$ , there was only a 16% decrease in the yield of **3a** when  $[\text{Cu}(\text{L4})_2]\text{PF}_6$  was used as the catalyst (Table 1, entry 16).

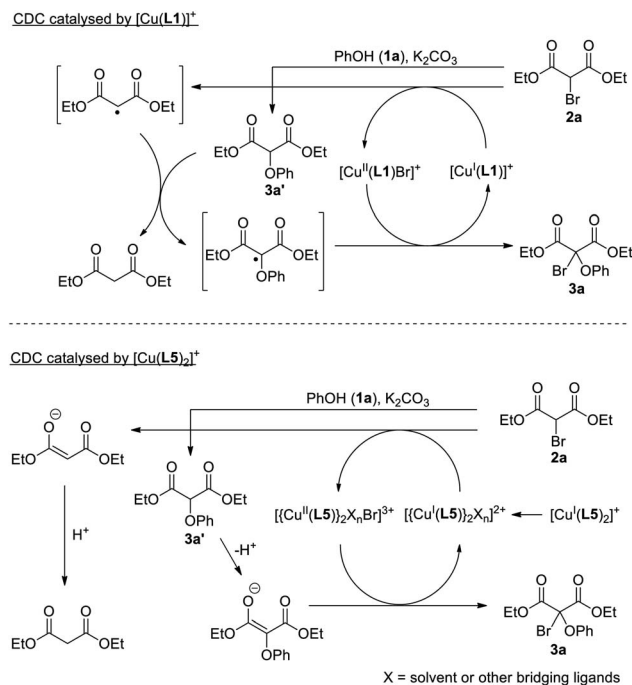


**Fig. 2** Proposed mechanisms of CDC catalysed by  $[\text{Cu}(\text{L1})]\text{PF}_6$  (above) and  $[\text{Cu}(\text{L5})_2]\text{PF}_6$  (below).

Further comparison of the effect of the catalyst loading also showed a great contrast between  $[\text{Cu}(\text{L4})_2]\text{PF}_6$  and  $[\text{Cu}(\text{L1})]\text{PF}_6$ . The CDC product **3a** was obtained in only 35% yield when 0.005 mol% of  $[\text{Cu}(\text{L4})_2]\text{PF}_6$  was used, suggesting that the non-interlocked complex could be more susceptible to non-productive side reactions and/or degradation (Table 1, entry 17). Interestingly, the presence of 1 eq. of TEMPO increased the yield of **3a** to 70% when  $[\text{Cu}(\text{L5})_2]\text{PF}_6$  was used as the catalyst (Table 1, entry 18). The opposite effect of the radical scavenger hence suggests the copper-catalysed CDC proceed *via* different pathways for the mechanically interlocked and non-interlocked systems. ESI-MS analysis of a reaction mixture of **1a** and **2a** with  $[\text{Cu}(\text{L5})_2]\text{PF}_6$  as the catalyst showed the presence of binuclear copper species such as  $[\text{Cu}_2^{\text{II,II}}(\text{L5})_2(\text{HCOO})_2(\text{OH})]^+$  at  $m/z = 649.2$  and  $[\text{Cu}_2^{\text{I,I}}(\text{L5})_2(\text{MeCN})_2\text{Br}]^+$  at  $m/z = 703.4$  (Fig. S3†). A bimetallic mechanism that involves an enolate is proposed, which is also supported by a preliminary DFT study (Fig. 2b). A similar binuclear mechanism has also been proposed for a related enolate chlorination.<sup>30</sup> Furthermore, a time-dependent study on **3a** formation catalysed by  $[\text{Cu}(\text{L5})_2]\text{PF}_6$  showed that the reaction was completed by a much shorter time (*ca.* 6 hours) than that by  $[\text{Cu}(\text{L1})]\text{PF}_6$  (*ca.* 20 hours), further reinforcing that the non-interlocked ligands may render the (binuclear) active copper species more susceptible to side reactions or catalyst degradation (Fig. S5†). Altogether, these results not only highlight again the efficiency and applicability of the catenane-coordinated copper in the new  $\text{C}(\text{sp}^3)\text{-O}$  cross coupling of phenols and bromodicarbonyls, but also demonstrate the advantages of a dynamic copper coordination site that is enabled by the strong and flexible mechanical bond in the catenane ligands.





Table 2 Substrate scope of the CDC<sup>a</sup>

Reaction scheme showing the synthesis of CDCs (3) from phenols (1) and bromodicarbonyl compounds (2) using 1 mol% [Cu(L1)]PF<sub>6</sub>, 2 eq. K<sub>2</sub>CO<sub>3</sub>, MeCN, 50 °C, air.

#### entry 1-4

3a: R<sup>1</sup> = R<sup>2</sup> = OEt, 90%  
 3b: R<sup>1</sup> = R<sup>2</sup> = OMe, 91%  
 3c: R<sup>1</sup> = R<sup>2</sup> = O<sup>t</sup>Bu, 90%  
 3d: R<sup>1</sup> = R<sup>2</sup> = OBn, 85%

#### entry 5

3e, 81%

#### entry 6

3f, 83%

#### entry 7-12

3g: R = F, 86%  
 3h: R = OMe, 92%  
 3i: R = OBn, 81%<sup>a</sup>  
 3j: R = Me, 96%  
 3k: R = Et, 94%  
 3l: R = <sup>t</sup>Bu, 88%

#### entry 13

3m, 78%<sup>b</sup>

#### entry 14

3n, 80%<sup>b</sup>

#### entry 15

3o, 85%<sup>b</sup>

#### entry 16

3p, 90%<sup>b</sup>

#### entry 17

3q, 72%

#### entry 18

3r, 92%

#### entry 19

3s, 88%<sup>b</sup>

#### entry 20

3t, 75%<sup>b</sup>

<sup>a</sup> Reactions are performed with **1a** (0.1 mmol) and **2a** (0.22 mmol) in 0.5 mL MeCN for 24 h. Presented are isolated yields. <sup>b</sup> The phenol substrates are easily air-oxidized and the reactions were performed under argon.

To put the C(sp<sup>3</sup>)-O dehydrogenative coupling in a synthetic and application perspective, the scope of the CDC catalysed by [Cu(L1)]PF<sub>6</sub> with various phenol and bromodicarbonyl substrates was investigated. As shown in Table 2, different bromomalonates, β-ketoester and 1,3-diketone, as well as phenols with either electron-rich or electron-deficient substituents, were found to give good yields of the coupling products (Table 2, entries 1–15). Moreover, multiple substituted phenols, including those with bulky *ortho*-substituents (e.g. –NO<sub>2</sub> and –<sup>t</sup>Bu), performed equally well in the CDC (Table 2, entries 16–19), demonstrating a wide substrate scope of the CDC. When catechol was used as the phenolic substrate, a double substituted five-membered ring product was obtained (Table 2, entry 20). Due to the importance of phenol/catechol analogues in naturally occurring small molecules and smart materials, this wide substrate scope will have strong implications in the synthesis of natural products, agrochemicals and pharmaceuticals with good step and atom economy. In fact, the CDC products can serve as an efficient precursor to imidazo[1,2-*b*]

pyridazines, which have been demonstrated as a potent pharmacophore for inhibiting the pro-inflammatory cytokine tumor necrosis factor α (TNF-α) for treating a diverse range of inflammatory, infectious and malignant conditions.<sup>31</sup> For example, compound **3e**, obtained in 81% yield from the corresponding CDC catalysed by [Cu(L1)]PF<sub>6</sub>, can be converted in two simple steps to chloroimidazo[1,2-*b*]pyridazine **5** that can be further functionalised to give various drug candidates for targeting TNF-α (Fig. 3).<sup>32</sup>

## Conclusions

In conclusion, the use of a catenane ligand to support a copper catalyst for the cross dehydrogenative C(sp<sup>3</sup>)-O coupling of phenols and bromodicarbonyls is reported. The flexible and strong mechanical bond in the catenane creates a dynamic and responsive copper coordination environment, such that the catalytically active state is available only transiently when substrate transformation is to be mediated by the metal, or otherwise a stable, coordinatively saturated resting state is maintained. The CDC catalysed by [Cu(L1)]PF<sub>6</sub> is highly efficient with a low catalyst loading and a wide substrate scope, and the catalyst can be employed in a gram-scale transformation without a significant loss in its catalytic efficiency.

The phenanthroline-derived copper catenanes used in this work are one of the most classical types of MIMs obtained from a templated synthesis. MIMs synthesis based on other transition metal templates with different coordination properties are also well developed, and incorporating a mechanical bond in metal complexes is therefore no longer considered as a forbidden task. With the newly discovered C(sp<sup>3</sup>)-O cross coupling activity in our copper catenanes, it can be envisioned that mechanical interlocking of coordination ligand will be a promising direction for exploiting the unique properties of mechanical bond in the development of next generation transition metal catalysts. More studies on catenane ligands and related MIMs for catalytic applications are currently underway in our laboratory.

## Conflicts of interest

There are no conflicts to declare.

## Acknowledgements

This work is supported by the Croucher Foundation. We acknowledge UGC funding administered by The University of Hong Kong for support of the Electrospray Ionization Quadrupole Time-of-Flight Mass Spectrometry Facilities under the support for Interdisciplinary Research in Chemical Science. We thank Dr Vanessa K.-Y. Lo and Prof. C. M. Che for helpful discussion.

## Notes and references

- For selected reviews, see: (a) G. Evano and N. Blanchard *Copper Mediated Cross-Coupling Reactions*, John Wiley &

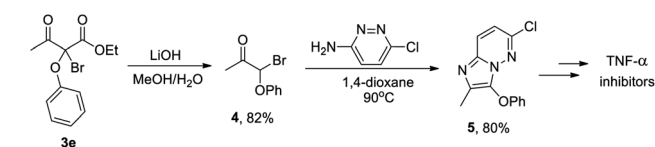


Fig. 3 Conversion of the CDC product **3e** to imidazo[1,2-*b*]pyridazine **5**.



- Sons Inc., New Jersey, 2013; (b) I. P. Beletskaya and A. V. Cheprakov, *Coord. Chem. Rev.*, 2004, **248**, 2337; (c) G. Evano, N. Blanchard and M. Toumi, *Chem. Rev.*, 2008, **108**, 3054; (d) H. Prokopcova and C. O. Kappe, *Angew. Chem., Int. Ed.*, 2008, **47**, 3674; (e) D. S. Surry and S. L. Buchwald, *Chem. Sci.*, 2010, **1**, 13; (f) G. Evano, C. Theunissen and A. Pradal, *Nat. Prod. Rep.*, 2013, **30**, 1467; (g) A. Casitas and X. Ribas, *Chem. Sci.*, 2013, **4**, 2301; (h) S. Bhunia, G. G. Pawar, S. V. Kumar, Y. Jiang and D. Ma, *Angew. Chem., Int. Ed.*, 2017, **56**, 16136; (i) A. Hossain, A. Bhattacharyya and O. Reiser, *Science*, 2019, **364**, eaav9713.
- 2 (a) D. R. McMillin and K. M. McNett, *Chem. Rev.*, 1998, **98**, 1201; (b) S.-J. Li and Y. Lan, *Chem. Commun.*, 2020, **56**, 6609; (c) H.-J. Himmel, *Inorg. Chim. Acta*, 2018, **481**, 56.
- 3 (a) A. J. Clark, *Eur. J. Org. Chem.*, 2016, 2231; (b) T. Pintauer and K. Matyjaszewski, *Chem. Soc. Rev.*, 2008, **37**, 1087; (c) W. T. Eckenhoff and T. Pintauer, *Catal. Rev.*, 2010, **52**, 1.
- 4 For examples of phenanthroline-supported, coordinatively saturated copper-based coupling catalysts: (a) A. Hossain, S. Engl, E. Lutscher and O. Reiser, *ACS Catal.*, 2019, **9**, 1103; (b) T. Rawner, E. Lutscher, C. A. Kaiser and O. Reiser, *ACS Catal.*, 2018, **8**, 3950.
- 5 (a) G. R. Jones, A. Anastasaki, R. Whitfield, N. Engelis, E. Liarou and D. M. Haddleton, *Angew. Chem., Int. Ed.*, 2018, **57**, 10468; (b) A. E. Wendlandt, A. M. Suess and S. S. Stahl, *Angew. Chem., Int. Ed.*, 2011, **50**, 11062; (c) R. Trammell, K. Rajabimoghadam and I. Garcia-Bosch, *Chem. Rev.*, 2019, **119**, 2954; (d) S. Iwamatsu, K. Matsubara and H. Nagashima, *J. Org. Chem.*, 1999, **64**, 9625.
- 6 For examples of copper catalysts of a low coordination number, see: (a) S. Wiese, Y. M. Badieli, R. T. Gephart, S. Mossin, M. S. Varonka, M. M. Melzer, K. Meyer, T. R. Cundari and T. H. Warren, *Angew. Chem., Int. Ed.*, 2010, **49**, 8850; (b) X. Ribas, C. Calle, A. Poater, A. Casitas, L. Gómez, R. Xifra, T. Parella, J. Benet-Buchholz, A. Schweiger, G. Mitrikas, M. Sola, A. Llobet and T. D. P. Stack, *J. Am. Chem. Soc.*, 2010, **132**, 12299; (c) X. Ribas, D. A. Jackson, B. Donnadiou, J. Mahla, T. Parella, R. Xifra, B. Hedman, K. O. Hodgson, A. Llobet and T. D. P. Stack, *Angew. Chem., Int. Ed.*, 2002, **41**, 2991; (d) Q. Zhang, Y. Liu, T. Wang, X. Zhang, C. Long, Y.-D. Wu and M.-X. Wang, *J. Am. Chem. Soc.*, 2018, **140**, 5579.
- 7 (a) W. Kaim, K. Beyer, V. Filippou and S. Zális, *Coord. Chem. Rev.*, 2018, **355**, 173; (b) Z. Weng, S. Teo and T. S. A. Hor, *Acc. Chem. Res.*, 2007, **40**, 676; (c) P. Braunstein and F. Naud, *Angew. Chem., Int. Ed.*, 2001, **40**, 680; (d) V. V. Grushin, *Chem. Rev.*, 2004, **104**, 1629; (e) C. S. Slone, D. A. Weinberger and C. A. Mirkin, *Prog. Inorg. Chem.*, 1999, **48**, 233.
- 8 For examples of MIMs as metal coordination ligands: (a) Y. Suzuki, K. Shimada, E. Chihara, T. Saito, Y. Tsuchido and K. Osakada, *Org. Lett.*, 2011, **13**, 3774; (b) G. Hattori, T. Hori, Y. Miyake and Y. Nishibayashi, *J. Am. Chem. Soc.*, 2007, **129**, 12930; (c) Y. Li, Y. Feng, Y.-M. He, F. Chen, J. Pan and Q.-H. Fan, *Tetrahedron Lett.*, 2008, **49**, 2878; (d) M. Yamazaki, T. Hagiwara, M. Sekiguchi, T. Sawaguchi and S. Yano, *Synth. Commun.*, 2008, **38**, 553.
- 9 (a) C. O. Dietrich-Buchecker, J. M. Kern and J.-P. Sauvage, *J. Chem. Soc., Chem. Commun.*, 1985, 760; (b) A. M. Albrecht-Gary, Z. Saad, C. O. Dietrich-Buchecker and J.-P. Sauvage, *J. Am. Chem. Soc.*, 1985, **107**, 3205; (c) M. Cirulli, A. Kaur, J. E. M. Lewis, Z. Zhang, J. A. Kitchen, S. M. Goldup and M. M. Roessler, *J. Am. Chem. Soc.*, 2019, **141**, 879.
- 10 For examples of stimuli-triggered (co)conformational change of metal-containing MIMs: (a) A. Livoreil, C. O. Dietrich-Buchecker and J.-P. Sauvage, *J. Am. Chem. Soc.*, 1994, **116**, 9399; (b) D. J. Cárdenas, A. Livoreil and J.-P. Sauvage, *J. Am. Chem. Soc.*, 1996, **118**, 11980; (c) D. A. Leigh, P. J. Lusby, A. M. Z. Slawin and D. B. Walker, *Chem. Commun.*, 2005, 4919; (d) F. Baumann, A. Livoreil, W. Kaim and J.-P. Sauvage, *Chem. Commun.*, 1997, 35; (e) P. Mobian, J.-M. Kern and J.-P. Sauvage, *Angew. Chem., Int. Ed.*, 2004, **43**, 2392; (f) A. Livoreil, J.-P. Sauvage, N. Armaroli, V. Balzani, L. Flamigni and B. Ventura, *J. Am. Chem. Soc.*, 1997, **119**, 12114.
- 11 For examples of reactive species stabilization by MIMs: (a) C. Dietrich-Buchecker, J.-P. Sauvage and J. M. Kern, *J. Am. Chem. Soc.*, 1989, **111**, 7791; (b) N. Armaroli, L. De Cola, V. Balzani, J.-P. Sauvage, C. O. Dietrich-Buchecker, J.-M. Kern and A. Bailal, *J. Chem. Soc., Dalton Trans.*, 1993, **21**, 3241; (c) H. Li, A. C. Fahrenbach, B. M. Savoie, C. Ke, J. C. Barnes, J. Lei, Y.-L. Zhao, L. M. Lilley, T. J. Marks, M. A. Ratner and J. F. Stoddart, *J. Am. Chem. Soc.*, 2013, **135**, 456; (d) M. Frascioni, T. Kikuchi, D. Cao, Y. Wu, W.-G. Liu, S. M. Dyar, G. Barin, A. A. Sarjeant, C. L. Stern, R. Carmieli, C. Wang, M. R. Wasielewski, W. A. Goddard III and J. F. Stoddart, *J. Am. Chem. Soc.*, 2014, **136**, 11011.
- 12 For examples of copper-templated catenane synthesis: (a) C. O. Dietrich-Buchecker, J.-P. Sauvage and J. P. Kintzinger, *Tetrahedron Lett.*, 1983, **24**, 5095; (b) C. O. Dietrich-Buchecker, J.-P. Sauvage and J. P. Kintzinger, *J. Am. Chem. Soc.*, 1984, **106**, 3043; (c) B. Mohr, M. Weck, J.-P. Sauvage and R. H. Grubbs, *Angew. Chem., Int. Ed.*, 1997, **36**, 1308; (d) J. D. Megiatto and D. I. Schuster, *J. Am. Chem. Soc.*, 2008, **130**, 12872; (e) S. M. Goldup, D. A. Leigh, T. Long, P. R. McGonigal, M. D. Symes and J. Wu, *J. Am. Chem. Soc.*, 2009, **131**, 15924; (f) J. D. Megiatto Jr, D. I. Schuster, S. Abwandner, G. de Miguel and D. M. Guldi, *J. Am. Chem. Soc.*, 2010, **132**, 3847; (g) J. A. Berrocal, M. M. L. Nieuwenhuizen, L. Mandolini, E. W. Meijer and S. D. Stefano, *Org. Biomol. Chem.*, 2014, **12**, 6167; (h) K.-L. Tong, C.-C. Yee, Y. C. Tse and H. Y. Au-Yeung, *Inorg. Chem. Front.*, 2016, **3**, 348; (i) R. Hayashi, P. Slavik, Y. Mutoh, T. Kasama and S. Saito, *J. Org. Chem.*, 2016, **81**, 1175.
- 13 (a) I. B. Krylov, V. A. Vil' and A. O. Terent'ev, *Beilstein J. Org. Chem.*, 2015, **11**, 92; (b) G. P. Maier, C. M. Bernt and A. Butler, *Biomater. Sci.*, 2018, **6**, 332; (c) Y. E. Lee, T. Cao, C. Torruellas and M. C. Kozlowski, *J. Am. Chem. Soc.*, 2014, **136**, 6782; (d) C. Yu and F. W. Patureau, *Angew. Chem., Int. Ed.*, 2018, **57**, 11807; (e) M. Uyanik, T. Mutsuga and K. Ishihara, *Angew. Chem., Int. Ed.*, 2017, **56**, 3956.



- 14 (a) S. A. Girard, T. Knauber and C.-J. Li, *Angew. Chem., Int. Ed.*, 2014, **53**, 74; (b) C. S. Yeung and V. M. Dong, *Chem. Rev.*, 2011, **111**, 1215; (c) H. Wang, X. Gao, Z. Lv, T. Abdelilah and A. Lei, *Chem. Rev.*, 2019, **119**, 6769; (d) Y. Qin, L. Zhu and S. Luo, *Chem. Rev.*, 2017, **117**, 9433.
- 15 C. Heiz, A. W. Jones, B. S. Oezkaya, C. L. Bub, M.-L. Louillat-Habermeyer, V. Wagner and F. W. Patureau, *Chem.-Eur. J.*, 2016, **22**, 17980.
- 16 W. Ali, S. K. Rout, S. Guin, A. Modi, A. Banerjee and B. K. Patel, *Adv. Synth. Catal.*, 2015, **357**, 515.
- 17 Y.-B. Wu, D. Xie, Z.-L. Zang, C.-H. Zhou and G.-X. Cai, *Chem. Commun.*, 2018, **54**, 4437.
- 18 W. Xu, Z. Huang, X. Ji and J.-P. Lumb, *ACS Catal.*, 2019, **9**, 3800.
- 19 (a) M. Uyanik, H. Okamoto, T. Yasui and K. Ishihara, *Science*, 2010, **328**, 1376; (b) M. Uyanik, H. Hayashi and K. Ishihara, *Science*, 2014, **345**, 291; (c) W. Xu and B. J. Nachtsheim, *Org. Lett.*, 2015, **17**, 1585; (d) M. Uyanik, K. Nishioka, R. Kondo and K. Ishihara, *Nat. Chem.*, 2020, **12**, 353.
- 20 I. B. Krylov, E. R. Lopat'eva, A. S. Budnikov, G. I. Nikishin and A. O. Terent'ev, *J. Org. Chem.*, 2020, **85**, 1935.
- 21 (a) H. Y. Au-Yeung, C.-C. Yee, A. W. H. Ng and K. Hu, *Inorg. Chem.*, 2018, **57**, 3475; (b) K. Wang, C.-C. Yee and H. Y. Au-Yeung, *Chem. Sci.*, 2016, **7**, 2787; (c) A. W. H. Ng, C.-C. Yee and H. Y. Au-Yeung, *Angew. Chem., Int. Ed.*, 2019, **58**, 17375.
- 22 For examples of the effects of the mechanical bond tightness on the MIMs properties: (a) A. Krueve, K. Caprice, R. Lavendomme, J. M. Wollschläger, S. Schoder, H. V. Schröder, J. R. Nitschke, F. B. L. Cougnon and C. A. Schalley, *Angew. Chem., Int. Ed.*, 2019, **58**, 11324; (b) K. Caprice, A. Aster, F. B. L. Cougnon and T. Kumpulainen, *Chem.-Eur. J.*, 2020, **26**, 1576.
- 23 For reviews on applications of MIMs in catalysis: (a) A. Martinez-Cuezva, A. Saura-Sanmartin, M. Alajarin and J. Berna, *ACS Catal.*, 2020, **10**, 7719; (b) E. A. Neal and S. M. Goldup, *Chem. Commun.*, 2014, **50**, 5128.
- 24 For examples of switchable MIM-based catalysts: (a) J. Berná, M. Alajarin and R.-A. Orenes, *J. Am. Chem. Soc.*, 2010, **132**, 10741; (b) V. Blanco, A. Carlone, K. D. Hänni, D. A. Leigh and B. Lewandowski, *Angew. Chem., Int. Ed.*, 2012, **51**, 5166; (c) V. Blanco, D. A. Leigh, U. Lewandowski, B. Lewandowski and V. Marcos, *J. Am. Chem. Soc.*, 2014, **136**, 15775; (d) J. Beswick, V. Blanco, G. De Bo, D. A. Leigh, U. Lewandowski, B. Lewandowski and K. Mishihiro, *Chem. Sci.*, 2015, **6**, 140; (e) K. Eichstaedt, J. Jaramillo-Garcia, D. A. Leigh, V. Marcos, S. Pisano and T. A. Singleton, *J. Am. Chem. Soc.*, 2017, **139**, 9376; (f) C.-S. Kwan, A. S. C. Chan and K. C.-F. Leung, *Org. Lett.*, 2016, **18**, 976; (g) A. Martinez-Cuezva, A. Saura-Sanmartin, T. Nicolas-Garcia, C. Navarro, R.-A. Orenes, M. Alajarina and J. Berna, *Chem. Sci.*, 2017, **8**, 3775.
- 25 For examples of MIM-based asymmetric catalysis: (a) Y. Tachibana, N. Kihara and T. Takata, *J. Am. Chem. Soc.*, 2004, **126**, 3438; (b) V. Blanco, D. A. Leigh, V. Marcos, J. A. Morales-Serna and A. L. Nussbaumer, *J. Am. Chem. Soc.*, 2014, **136**, 4905; (c) S. Hoekman, M. O. Kitching, D. A. Leigh, M. Papmeyer and D. Roke, *J. Am. Chem. Soc.*, 2015, **137**, 7656; (d) M. Galli, J. E. M. Lewis and S. M. Goldup, *Angew. Chem., Int. Ed.*, 2015, **54**, 13545; (e) G. Gil-Ramírez, S. Hoekman, M. O. Kitching, D. A. Leigh, I. J. Victorica-Yrezabal and G. Zhang, *J. Am. Chem. Soc.*, 2016, **138**, 13159; (f) K. Xu, K. Nakazono and T. Takata, *Chem. Lett.*, 2016, **45**, 1274; (g) Y. Cakmak, S. Erbas-Cakmak and D. A. Leigh, *J. Am. Chem. Soc.*, 2016, **138**, 1749; (h) R. Mitra, H. Zhu, S. Grimme and J. Niemeyer, *Angew. Chem., Int. Ed.*, 2017, **56**, 11456; (i) A. Martinez-Cuezva, M. Marin-Luna, D. A. Alonso, D. Ros-Ñiguez, M. Alajarin and J. Berna, *Org. Lett.*, 2019, **21**, 5192; (j) M. Dommaschk, J. Echavarren, D. A. Leigh, V. Marcos and T. A. Singleton, *Angew. Chem., Int. Ed.*, 2019, **58**, 14955; (k) A. W. Heard and S. M. Goldup, *Chem*, 2020, **6**, 994; (l) N. Pairault, H. Zhu, D. Jansen, A. Huber, C. G. Daniliuc, S. Grimme and J. Niemeyer, *Angew. Chem., Int. Ed.*, 2020, **59**, 5102.
- 26 (a) V. Marcos, A. J. Stephens, J. Jaramillo-Garcia, A. L. Nussbaumer, S. L. Woltering, A. Valero, J.-F. Lemonnier, I. J. Victorica-Yrezabal and D. A. Leigh, *Science*, 2016, **352**, 1555; (b) T. Prakasam, A. Devaraj, R. Saha, M. Lusi, J. Brandel, D. Esteban-Gomez, C. Platas-Iglesias, M. A. Olson, P. S. Mukherjee and A. Trabolsi, *ACS Catal.*, 2019, **9**, 1907.
- 27 C.-C. Yee, A. W. H. Ng and H. Y. Au-Yeung, *Chem. Commun.*, 2019, **55**, 6169.
- 28 (a) J. B. Niederl and R. T. Roth, *J. Am. Chem. Soc.*, 1940, **62**, 1154; (b) K. H. Takemura, M. Pulickal and F. O. Hoff, *J. Org. Chem.*, 1971, **36**, 3646.
- 29 (a) R. C. Walroth, K. C. Miles, J. T. Lukens, S. N. MacMillan, S. S. Stahl and K. M. Lancaster, *J. Am. Chem. Soc.*, 2017, **139**, 13507; (b) M. M. Hossaina and S.-G. Shyua, *Adv. Synth. Catal.*, 2010, **352**, 3061.
- 30 (a) E. M. Kosower and G.-S. Wu, *J. Org. Chem.*, 1963, **28**, 633; (b) J. S. Sharley, A. M. Collado Pérez, E. E. Ferri, A. F. Miranda and I. R. Baxendale, *Tetrahedron*, 2016, **72**, 2947.
- 31 (a) S. S. Pandit, M. R. Kulkarni, U. Ghosh, Y. B. Pandit and N. P. Lad, *Mol. Diversity*, 2018, **22**, 545; (b) S. S. Pandit, M. R. Kulkarni, Y. B. Pandit, N. P. Lad and V. M. Khedkar, *Bioorg. Med. Chem. Lett.*, 2018, **28**, 24.
- 32 M. H. Ali, D. C. Brookings, J. A. Brown, M. C. Hutchings, V. E. Jackson, B. Kroepfien, J. R. Porter and J. R. Quincey, *US Pat.*, 9873703, 2015.

